

## Revisiting of dimensional scaling of linear chains in dilute solutions

Fei Hong<sup>a</sup>, Yijie Lu<sup>a</sup>, Junfang Li<sup>a</sup>, Wenjing Shi<sup>a</sup>, Guangzhao Zhang<sup>a,\*</sup>, Chi Wu<sup>a,b,\*\*</sup>

<sup>a</sup>Hefei National Laboratory for Physical Sciences at Microscale, Department of Chemical Physics, University of Science and Technology of China, Hefei, Anhui 230026, China

<sup>b</sup>Department of Chemistry, The Chinese University of Hong Kong, Shatin, N.T., Hong Kong

### ARTICLE INFO

#### Article history:

Received 17 October 2009

Received in revised form

11 January 2010

Accepted 17 January 2010

Available online 25 January 2010

#### Keywords:

Polystyrene

Dimensional scaling

Laser light-scattering

### ABSTRACT

The dimensions of linear polymer chains are scaled to their molar mass ( $M$ ) as  $R = kM^\alpha$  with  $\alpha = 1/2$  and  $3/5$  in a theta and an athermal solvent, respectively. In a good solvent, both  $k$  and  $\alpha$  are a function of the solvent quality and chain length range. A high-temperature laser light-scattering spectrometer was used to measure the average radius of gyration ( $\langle R_g \rangle$ ) and hydrodynamic radius ( $\langle R_h \rangle$ ) of a set of narrowly distributed linear polystyrene chains in decalin over a wide temperature range.  $k$  and  $\alpha$  in the scaling experimentally varying with  $T$  over a chain length range was analyzed. The results reveal that for  $\langle R_g \rangle$ ,  $\alpha = 0.59 - 0.09\exp(-\tau/0.066)$  and  $k = 0.60\tau^{2\alpha-1}$ , reasonably agreeing with the thermal blob theory. For  $\langle R_h \rangle$ ,  $\alpha = 0.59 - 0.09\exp(-\tau/0.106)$ , but  $k$  deviates from the relationship of  $k \propto \tau^{2\alpha-1}$ , reflecting that the hydrodynamic interaction and chain draining are not considered in the thermal blob theory.

Crown Copyright © 2010 Published by Elsevier Ltd. All rights reserved.

### 1. Introduction

It has been well known that the root-mean-square end-to-end distance ( $R_0$ ) of linear flexible chains in dilute solutions can be scaled to the number of thermal blobs ( $N_b$ ) as [1]:

$$R_0 \cong \xi_T N_b^\alpha \quad (1)$$

where  $\alpha$  is the scaling exponent and  $\xi_T$  is the dimension of each thermal blob. Both of them are constants for a certain polymer solution at a given temperature. In the thermal blob theory [2], each blob contains  $n_k$  Kuhn segments and  $N_b = N_k/n_k$ , where  $N_k$  is the number of the Kuhn segments per chain.  $\xi_T$  is proportional to the Kuhn length ( $b$ ) and inversely proportional to the reduced temperature ( $\tau = (T - \theta)/T$ ), using the Flory  $\theta$  temperature as a reference point; namely,

$$\xi_T \sim b/\tau \quad (2)$$

On a scale shorter than  $\xi_T$ , the sub-chain inside each blob follows the random-walk statistics and the three-body interaction dominates; namely,  $\xi_T = bn_k^{1/2}$  or  $n_k \sim 1/\tau^2$ . While on a scale longer than  $\xi_T$ , the two-body excluded volume effect becomes important. In the  $\theta$ -solvent,  $\tau = 0$  and  $\alpha = 1/2$ , so that the entire chain has a random-coil

conformation. In an athermal solvent,  $\tau \rightarrow 1$  (i.e.,  $T \rightarrow \infty$ ),  $\alpha \rightarrow 3/5$ , so that the chain segments are fully excluded from each other in the scale longer than  $b$ . In other words, the excluded volume interaction is statistically assumed to be a step function. In reality, each coiled linear chain undergoes a self-avoiding random-walk of thermal blobs between these two limits. The two extreme regions are distinguished by  $n_k$ , a cut-off parameter. Therefore,  $R_0$  is related to  $b$ ,  $\tau$  and  $N$  as:

$$R_0 = bN_k^{1/2} \text{ for } N_k < n_k \text{ and } R_0 \sim b\tau^{1/5}N_k^{3/5} \text{ for } N_k > n_k \quad (3)$$

Experimentally, a change of the solution temperature can switch a polymer solution between these two extreme states, resulting in a variation of  $\alpha$  between  $1/2$  and  $3/5$ . Quantitatively, how  $\alpha$  and  $k$  varying with  $\tau$  are still missing. Note that the hydrodynamic interaction length is not considered in the blob theory. Actually, both the solvent quality and chain length affect the hydrodynamic draining. It might be difficult to solve these problems using the current blob model, but we can try to experimentally establish some empirical functional forms to elucidate the transition between the two extreme states: the  $\theta$ - and athermal solvents.

However, such a powerful scaling analysis of linear polymer chains in dilute solutions has been used to study a range of solution properties, such as the average hydrodynamic radius ( $\langle R_h \rangle$ ) [3, 4], the average radius of gyration ( $\langle R_g \rangle$ ) [5, 6], the second virial coefficient ( $A_2$ ) [7] and the expansion factor ( $\sigma$ ) [8]. In 1997, Colby [9] as well as Rai and Rosen [10] studied the temperature dependent scaling between the intrinsic viscosity and the chain length using the thermal blob theory. Previously, a large number of

\* Corresponding author. Tel./fax: +86 551 3606763.

\*\* Corresponding author. Hefei National Laboratory for Physical Sciences at Microscale, Department of Chemical Physics, University of Science and Technology of China, Hefei, Anhui 230026, China.

E-mail address: [gzzhang@ustc.edu.cn](mailto:gzzhang@ustc.edu.cn) (G. Zhang).

experimentally measured values of  $\langle R_g \rangle$  and  $\langle R_h \rangle$  of different polymers in various solvents have been accumulated over the past three decades. Unfortunately, these existing data cannot be used to elucidate how  $\alpha$  and  $k$  depend on the solution temperature because most of the data were collected in different solvents and either the chain length or the temperature range is not sufficiently wide. For example,  $\tau$  is typically smaller than 0.1.

In a recent new book, Rubinstein and Colby [11] used static light-scattering data of different polymer solutions over a wide temperature range collected by Berry more than 40 years ago [12]. However, a systematic variation of the temperature for each polymer solution is still missing. Namely, there are no  $\langle R_g \rangle$  values of a set of polymer chains with different lengths over a set of given solution temperatures. This leads us to revisit this old problem; namely, the temperature dependence of  $\langle R_g \rangle$  and  $\langle R_h \rangle$  of a set of narrowly distributed linear chains with different lengths over a wide temperature range. Our sole objective is to find how  $\alpha$  and  $k$  are related to  $\tau$  and hope to find some general relationship so that we are able to predict the chain dimension of a given linear polymer in dilute solutions from its length and the reduced temperature, independent of the nature of monomer and solvent. In the current study, the selection of decalin as a solvent for polystyrene is due to its extraordinarily wide temperature range (4–140 °C) that is reachable in our current high-temperature laser light-scattering spectrometer.

## 2. Experimental section

### 2.1. Materials

Five narrowly distributed polystyrene (PS) samples ( $M_w = 4.95 \times 10^5 - 1.19 \times 10^7$  g/mol) were prepared by the high-vacuum anionic living polymerization. Their molecular characterization results are listed in Table 1. The reagent-grade decalin from Aladdin was dried and further purified by fractional distillation [13]. For each PS sample, at least four solutions with different concentrations were prepared by diluting a stock solution. Each stock solution was stored at the room temperature for at least one week to ensure a complete dissolution, especially for those high molar mass samples. The concentration ranged from  $2.0 \times 10^{-5}$  to  $2.0 \times 10^{-3}$  g/L depending on the molecular weight of the sample. The solvent viscosity at different temperature was measured by Ubbelohde viscometer. Each solution was clarified with a 0.45- $\mu$ m Millipore Millex-LCR filter to remove dust particles prior to the light-scattering experiments.

### 2.2. Laser light-scattering

A commercial high-temperature LLS spectrometer (ALV/DLS/SLS-5022F) equipped with a multi- $\tau$  digital time correlation (ALV5000) and a cylindrical 22 mW UNIPHASE He-Ne laser ( $\lambda_0 = 632.8$  nm) as the light source was used. Its operative temperature range is 4–140 °C. The details of LLS instrumentation and theory can be found elsewhere [14, 15]. In static LLS, the weight-average molar mass ( $M_w$ ) and the z-average root-mean-

square radius of gyration ( $\langle R_g^2 \rangle^{1/2}$  or written as  $\langle R_g \rangle$ ) of linear polymer chains in a dilute solution can be determined from the angular dependence of the excess absolute time-averaged scattering intensity, known as the Rayleigh ratio  $R_{VV}(q)$ , on the basis of:

$$\frac{KC}{R_{VV}(q)} \cong \frac{1}{M_w} \left( 1 + \frac{1}{3} \langle R_g^2 \rangle q^2 \right) + 2A_2C \quad (4)$$

where  $K = 4\pi^2 n^2 (dn/dC)^2 / (N_A \lambda_0^4)$  and  $q = (4\pi n / \lambda_0) \sin(\theta/2)$  with  $n$ ,  $dn/dC$ ,  $N_A$ ,  $\lambda_0$ , and  $\theta$ , the solvent refractive index, the specific refractive index increment, the Avogadro's number, the wavelength of light in vacuum, and the scattering angle, respectively. The extrapolations of both  $C \rightarrow 0$  and  $q \rightarrow 0$  lead to  $M_w$ . The plots of  $[KC/R_{VV}(q)]_{C \rightarrow 0}$  vs  $q^2$  and  $[KC/R_{VV}(q)]_{q \rightarrow 0}$  vs  $C$  lead to  $\langle R_g^2 \rangle$  and  $A_2$ , respectively. In an extremely dilute solution, the term of  $2A_2C$  can be ignored. For relatively small scattering objects, the Zimm plot on the basis of eq. (3) incorporates the extrapolations of  $C \rightarrow 0$  and  $q \rightarrow 0$  in a single grid. For long polymer chains, i.e.,  $q\langle R_g \rangle > 1$ , the Berry plot is often used to obtain  $\langle R_g \rangle$ . In SLS, the measurement was done from 15 to 140° at each angle for three times, the average time is 30 s. The error was set under  $\pm 1\%$ .

In dynamic LLS [16], the cumulant analysis of each measured intensity-intensity time correlation function  $G^2(t)$  of narrowly distributed chains in a dilute solution is sufficient for an accurate determination of the average line width ( $\langle \Gamma \rangle$ ). For a diffusive relaxation,  $\langle \Gamma \rangle$  can be further related to the average translational diffusion coefficient ( $\langle D \rangle$ ) using  $\langle D \rangle = (\langle \Gamma \rangle / q^2)_{q \rightarrow 0, C \rightarrow 0}$  or the average hydrodynamic radius ( $\langle R_h \rangle$ ) using  $\langle R_h \rangle = k_B T / (6\pi\eta \langle D \rangle)$  with  $k_B$ ,  $\eta$ , and  $T$ , the Boltzmann constant, the solvent viscosity, and the absolute solution temperature, respectively. The hydrodynamic radius distribution  $f(R_h)$  can also be calculated for the Laplace inversion of  $G^2(t)$ . In the current study, the solution temperature was varied in the range 15–140 °C. The long-term temperature fluctuation inside the scattering cell is within  $\pm 0.1$  °C even at 140 °C.

## 3. Results and discussion

### 3.1. The theoretic background

As stated before, in the thermal blob theory [17–19], the universality is derived on the basis of the number of thermal blobs ( $N_b = N_k / n_k$ ), where  $N_k$  and  $n_k$  are numbers of Kuhn segments per chain and per thermal blob, respectively.  $n_k$  is a temperature dependent cut-off parameter, roughly distinguishing the Gaussian and excluded volume regimes. Akcasu and Han [19] showed:

$$N_b = \frac{N_k}{n_k} = \tau^2 \frac{N_p}{an} \quad (5)$$

where  $N_p$  is the degree of polymerization,  $n$  is the number of monomer per Kuhn segment and  $a$  is a constant, insensitive to types of monomer and solvent. For polystyrene, after matching experimental and theoretical results, they determined the values of  $an \cong 4$  in the range  $n \sim 15$ –20. Thus, they obtained  $a = 0.2$  when they chose  $n = 20$ . Note that  $n_k$  only depends on  $\tau$ , not on the total chain length.

### 3.2. Temperature ( $T$ ) and molecular weight ( $M_w$ ) dependences of $\langle R_g \rangle$

Using static LLS, we measured the temperature dependent average radius of gyration ( $\langle R_g \rangle$ ) of polystyrene samples with different chain lengths in decalin over a wide temperature range 15–140 °C. In the current study, the molar mass range  $4.91 \times 10^5 < M_w < 1.19 \times 10^7$  corresponds to  $1 \times 10^3 < N' < 3 \times 10^4$ , where  $N_p / (an)$  is defined as  $N'$ . Since  $\langle R_g \rangle \sim R_0$ , eq. (1) can be

**Table 1**  
Molecular parameters of the polystyrene samples.

Sample	$N_p$	$M_w$ (g/mol)	$M_w/M_n$	$N' = N_p/an$
PS1	$4.82 \times 10^3$	$5.01 \times 10^5$	1.06	$1.20 \times 10^3$
PS2	$9.00 \times 10^3$	$9.36 \times 10^5$	1.08	$2.25 \times 10^3$
PS3	$2.13 \times 10^4$	$2.21 \times 10^6$	1.08	$5.31 \times 10^3$
PS4	$3.60 \times 10^4$	$3.74 \times 10^6$	1.08	$9.00 \times 10^3$
PS5	$1.14 \times 10^5$	$1.19 \times 10^7$	1.09	$2.86 \times 10^4$

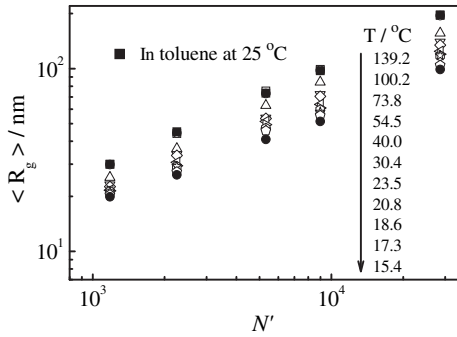


Fig. 1. Chain length dependence of average radius of gyration ( $\langle R_g \rangle$ ) of polystyrene samples at different temperatures in decalin, where  $\theta = 15.4^\circ\text{C}$ .

rewritten as  $\langle R_g \rangle = kN'^\alpha$  for each given  $\tau$ . Note that both  $k$  and  $\alpha$  vary with  $\tau$ . For each given  $\tau$ , we can obtain a set of  $k$  and  $\alpha$ . Therefore, Fig. 1 leads to the reduced temperature ( $\tau$ ) dependence of  $k_g(\tau)$  and  $\alpha_g(\tau)$ , where the subscript “g” denotes that both  $k$  and  $\alpha$  are from  $\langle R_g \rangle$  versus  $N'$ . Fig. 1 shows double logarithmical plots of  $\langle R_g \rangle$  versus  $N'$  from different  $\tau$  values, where we used polystyrene in toluene at the room temperature as a good solvent reference. A typical Zimm plot was shown in Fig. 2. From the plots of  $[KC/R_{vv}(q)]_{C \rightarrow 0}$  vs  $q^2$ , we obtained the average radius of gyration ( $\langle R_g \rangle$ ) of each sample at different temperature. It should be noted that according to the blob model, the scaling exponent  $\alpha$  should not be a constant when the solvent quality is between the two limits; namely,  $\alpha$  depends on the chain length range used. In this study, we have purposely chosen a molar mass range that is experimentally more relevant because for short chains LLS is not accurate to measure the radius of gyration. Here our main purpose is to experimentally elucidate how  $\alpha$  and  $k$  vary with the solvent quality for a meaningful chain length range that is more important in our daily experiments.

### 3.3. Scaling about temperature dependence of $\langle R_g \rangle$

Fig. 3 shows how  $\alpha_g$  increases with the reduced temperature ( $\tau$ ). At the  $\theta$  temperature ( $15.4^\circ\text{C}$ ,  $\tau = 0$ ) [20],  $\alpha_g = 0.500 \pm 0.005$ ; while at  $T = 139.2^\circ\text{C}$ ,  $\alpha_g = 0.587 \pm 0.005$ , fairly close to  $0.585 \pm 0.005$  in toluene. Note that as  $\tau \rightarrow 0.3$ ,  $\alpha_g \rightarrow 0.588$ , a theoretical limit in an athermal solution after the renormalization consideration [11, 21]. Ackasu and Han [19] estimated that for polystyrene in toluene,  $\theta \sim -41^\circ\text{C}$ ; namely,  $\tau$  only reaches 0.2 at the room temperature. The data in Fig. 3 can be represented by  $\alpha_g = A - B\exp(-\tau/T_C)$ . It has been known that at  $\tau = 0$  and 1,  $\alpha_g = 0.5$  and 0.588. Therefore, we can fix  $A = 0.59$  and  $B = 0.09$  and the fitting becomes a more reliable single parameter one. Our result shows that  $T_C = (6.6 \pm 0.3) \times 10^{-2}$ , where we only choose two significant digits because of some

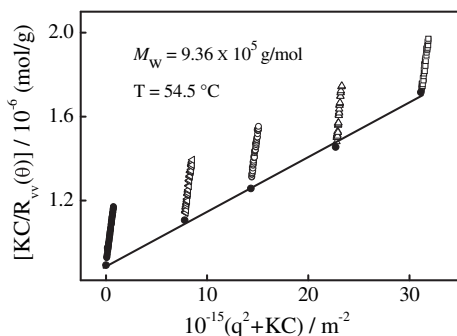


Fig. 2. Zimm plot of polystyrene with molecular weight of  $9.36 \times 10^5 \text{ g/mol}$  at  $54.5^\circ\text{C}$  in decalin.

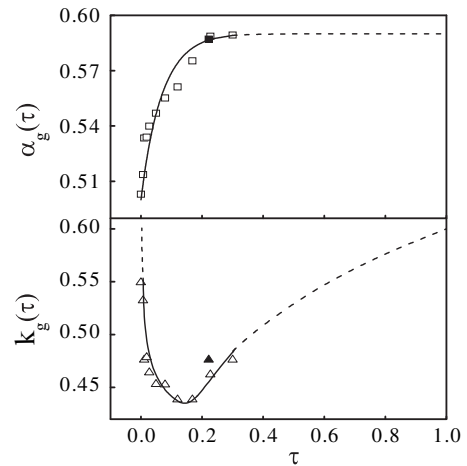


Fig. 3. Reduced temperature ( $\tau$ ) dependence of scaling exponent  $\alpha_g(\tau)$  and prefactor  $k_g(\tau)$  where the lines represent the least-square fitting of  $\alpha_g(\tau) = 0.59 - 0.09\exp(-\tau/0.066)$  and  $k_g(\tau) = 0.60\tau^{2\alpha-1}$ , respectively.

experimental uncertainties. On the other hand, using eq. (5) we can combine the two equations in eq. (3) into a general form as:

$$R_0 \cong \zeta_T \left( \frac{N_k}{n_k} \right)^\alpha = b\tau^{2\alpha-1}N'^\alpha \quad (6)$$

Therefore, we finally have  $k = k'\tau^{2\alpha-1}$ , where  $k'$  is a proportional constant since  $\langle R_g \rangle \propto R_0$ . The least-square fitting of “ $k_g(\tau)$  versus  $\tau$ ” in Fig. 3 results in  $k' = (6.0 \pm 0.6) \times 10^{-1}$ . To our knowledge, this is the first observed upturn of  $k$  as the solvent quality becomes better and better. Since  $n_k$  is insensitive to the types of monomer and solvent,  $k_g(\tau)$  and  $\alpha_g(\tau)$  obtained here would be applicable to other linear polymer chains in dilute solutions. Namely, we should be able to estimate  $\langle R_g \rangle$  of a linear polymer at any given temperature as long as  $\theta$  is known. Note that the unperturbed dimension also has temperature dependence. As we know, the radius of gyration ( $\langle R_g \rangle$ ) can be written as:

$$\langle R_g \rangle = \langle R_g \rangle_0(\tau)\alpha_S(\tau) = \langle R_g \rangle(\theta)F_0(\tau)\alpha_S(\tau) \quad (7)$$

where  $\langle R_g \rangle_0$  and  $\langle R_g \rangle(\theta)$  are the unperturbed dimension and the dimension at the  $\theta$  temperature, respectively.  $F_0(\tau)$  represents the temperature dependence of the unperturbed dimension, and  $\alpha_S(\tau)$  is the expansion factor. Thus, both  $\alpha_S(\tau)$  and  $\langle R_g \rangle_0$  have temperature dependence. Actually, Osa et al. [22] reported that the

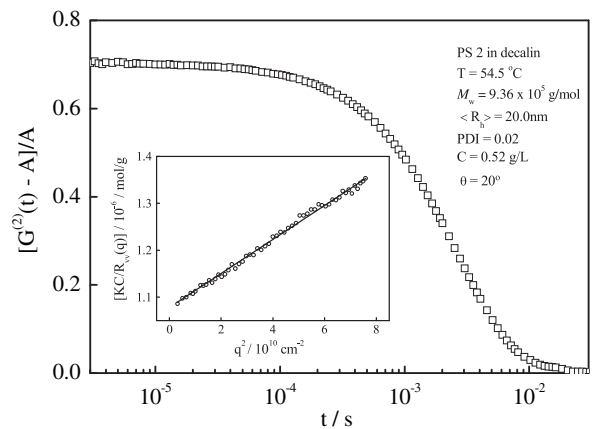
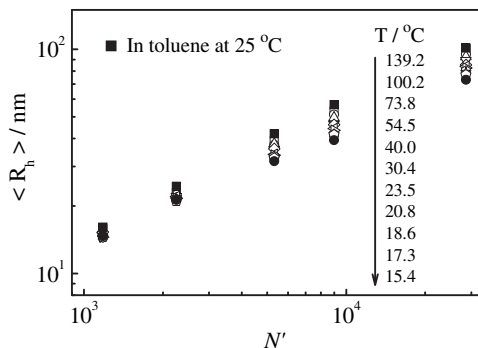


Fig. 4. Intensity–intensity time correlation functions of polystyrene with molecular weight of  $9.36 \times 10^5 \text{ g/mol}$  at  $54.5^\circ\text{C}$  in decalin. The inset is the angular dependence of the Rayleigh ratio  $[KC/R_{vv}(q)]$ .



**Fig. 5.** Chain length dependence of average hydrodynamic radius ( $\langle R_h \rangle$ ) of polystyrene samples at different temperatures in decalin, where  $\theta = 15.4^\circ\text{C}$ .

unperturbed dimension of polystyrene in a good solvent (toluene) or athermal solution drops as temperature increases. Here, because of the variation of  $F_0(\tau)$  cannot be estimated from the present experimental data, we cannot give the temperature dependence of  $\langle R_g \rangle_0$ .

Fig. 3 also shows  $\alpha_g(\tau)$  increases with temperature, and it is less than 3/5 at high-temperature. Note that we did not observe a crossover here, which is predicted by the blob theory. Curro and Schaefer [23, 24] have studied the temperature dependence of chain statistics by using small angle X-scattering and simulation, and they also did not observe such a crossover. It was attributed to the internal segment expansion effect, which was not considered in the blob theory. Actually, the crossover is observable only when the chain length becomes infinite and  $T \rightarrow 1$ . In real experiments, one never reaches such pre-conditions, especially for  $T \rightarrow 1$ . Therefore, the predicted crossover remains a challenge.

### 3.4. Temperature ( $T$ ) and molecular weight ( $M_w$ ) dependences of $\langle R_h \rangle$

On the other hand, using dynamic LLS, we measured the corresponding temperature dependent average hydrodynamic radius ( $\langle R_h \rangle$ ) at different angles over a wide temperature range. Fig. 4 shows a typical correlation function of PS2, the polydispersity index (PDI) obtained from the second order cumulant fitting is 0.02. The inset shows a typical angular dependence of the Rayleigh ratio [ $KC/R_{VV}(q)$ ] at 54.5 °C. The dynamic Zimm plot for each polystyrene

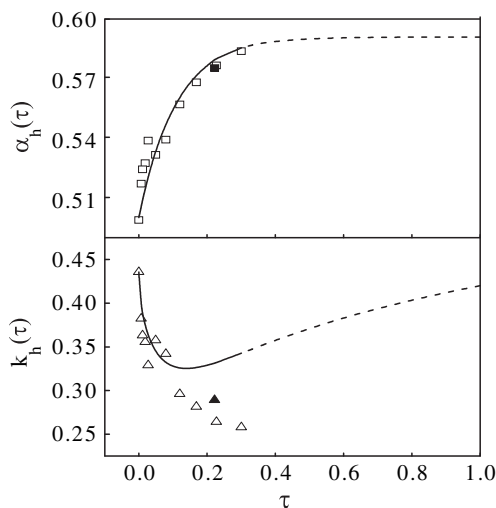


**Fig. 6.** Reduced temperature ( $\tau$ ) dependence of scaling exponent  $\alpha_h(\tau)$  and prefactor  $k_h(\tau)$ , where the lines represent the least-square fitting of  $\alpha_h(\tau) = 0.59 - 0.09\exp(-\tau/0.106)$  and  $k_h(\tau) = 0.42\tau^{2\alpha-1}$ , respectively.

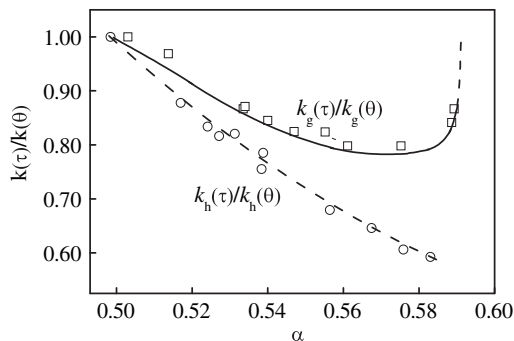


**Fig. 7.** Parametric plot of  $k(\tau)/k(\theta)$  as a function of scaling exponent  $\alpha$ , where subscripts “g” and “h” denoted that they were obtained from  $\langle R_g \rangle$  and  $\langle R_h \rangle$ , respectively; and the solid line represents  $\tau^{2\alpha-1}$ , while the dash line is just plotted to guide eyes.

sample and temperature leads to one average hydrodynamic radius ( $\langle R_h \rangle$ ) at  $C \rightarrow 0$  and  $q \rightarrow 0$ . Fig. 5 shows double logarithmical plots of  $\langle R_h \rangle$  against  $N'$  for five different PS samples in decalin at different solution temperatures. The least-square fitting of each set of data at a given temperature also leads to a pair of  $k_h(\tau)$  and  $\alpha_h(\tau)$  on the basis of eq. (1), where the subscript “h” denotes that they are obtained from the average hydrodynamic radius. The fitting of  $\alpha_h(\tau)$  versus  $\tau$  leads to  $T_C = (1.06 \pm 0.05) \times 10^{-1}$ , but the fitting of “ $k_h(\tau)$  versus  $\tau$ ” in Fig. 6 using  $k = k'\tau^{2\alpha-1}$  is fairly poor. Unlike in the case of  $R_g$ ,  $k_h(\tau)$  decrease as the solution temperature increases up to 140 °C and no upturn is observed. This is understandable because  $\langle R_h \rangle$  is of a hydrodynamic property and  $k_h(\tau)$  contains additional hydrodynamic interaction. As stated by Akcasu and Han [19],  $\langle R_h \rangle$  is not simply represented by the scaling of  $\langle R_h \rangle \sim N'^\alpha$  and the fitting of “ $\langle R_h \rangle$  versus  $N'$ ” into a power law results in a value of  $\alpha_h(\tau)$  lower than the predicted one. Such an obtained value of  $\alpha_h(\tau)$  depends on the range of chain length used. Our current result confirms it.

### 3.5. Relation between $k(\tau)/k(\theta)$ and $\alpha$

Fig. 7 shows a parametric plot of  $k(\tau)/k(\theta)$  versus  $\alpha$ . Eq. (3) indicates that in both the limits of the  $\theta$  and the athermal states ( $\alpha = 0.50$  and  $0.59$ ),  $k(\tau)/k(\theta)$  should approach unity. Therefore, there must be a minimum between these two limits. Note that the function of  $\tau^{2\alpha-1}$  has a minimum near  $\tau \sim 0.15$ , corresponding to  $\alpha \sim 0.58$  as predicted. In the range  $0 < \tau < 0.1$ ,  $k(\tau)$  decreases as  $\tau$  increases. Note that in most of previous experimental results,  $\tau < 0.1$  so that  $k(\tau)$  decreases as the solvent quality becomes better. To our knowledge, this might be the first experimental observation of the  $k(\tau)$  upturn at higher reduced temperatures. The gradual deviation of  $k_h(\tau)/k_h(\theta)$  from the predicted line might reflect that the chain becomes more draining because it swells at higher  $\tau$ . Finally, we emphasize that according to the blob model, both  $\alpha$  and  $k$  are functions of the chain length range and solvent quality.

## 4. Conclusion

By measuring the average radius of gyration ( $\langle R_g \rangle$ ) and hydrodynamic radius ( $\langle R_h \rangle$ ) of five narrowly distributed polystyrene samples with different lengths in decalin over a wide temperature range ( $15 < T < 140^\circ\text{C}$ ), we have obtained two empirical scalings for linear polymer chains in dilute solutions, covering the entire good solvent range from the  $\theta$  state to the athermal state over a more practical molar mass range. Namely,  $\langle R_g \rangle$  (nm) =  $0.60\tau^{2\alpha-1}N'^\alpha$  with  $\alpha = 0.59 - 0.09\exp(-\tau/6.6 \times 10^{-2})$  and  $\langle R_h \rangle$  (nm) =  $0.42\tau^{2\alpha-1}N'^\alpha$  with  $\alpha = 0.59 - 0.09\exp(-\tau/1.06 \times 10^{-1})$ , where  $N' = N_p/an$  with  $N_p$  and  $n$ , the degrees of polymerization per chain and per Kuhn segment, respectively; and  $a$  is a constant, insensitive to types of chain and

solvent. For polystyrene, in good solvents,  $an \cong 4$ . It is expected that such obtained scalings are applicable for other linear polymer chains in dilute solutions as long as the Flory  $\theta$  temperature is known because other parameters can be experimentally determined from a one-point measurement.

### Acknowledgment

The financial support of Ministry of Science and Technology of China (2007CB936401), the National Natural Scientific Foundation of China (NNSFC) Projects (50773077 and 20725414) and the Hong Kong Special Administration Region (HKSAR) Earmarked Project (CUHK4037/07P, 2160331) is gratefully acknowledged.

### Appendix. Supplementary material

Supplementary material associated with this article can be found, in the online version, at [doi:10.1016/j.polymer.2010.01.034](https://doi.org/10.1016/j.polymer.2010.01.034).

### References

- [1] de Gennes PG. *Macromolecules* 1976;9(4):587–93. 594–598.
- [2] de Gennes PG. *Scaling concepts in polymer physics*. NY: Cornell Univ Press; 1979.
- [3] Vidakovic P, Rondelez F. *Macromolecules* 1983;16(2):253–61.
- [4] Vidakovic P, Rondelez F. *Macromolecules* 1985;18(4):700–8.
- [5] Osa M, Yoshizaki T, Yamakawa H. *Macromolecules* 2000;33(13):4828–35.
- [6] Osa M, Sawatari N, Konishi T, Yoshizaki T, Yamakawa H. *Macromolecules* 1994;27(20):5697–703.
- [7] Takano A, Kushida Y, Ohta Y, Masuoka K, Matsushita Y. *Polymer* 2009;50(5):1300–3.
- [8] Yamakawa H. *Macromolecules* 1993;26(19):5061–6.
- [9] Colby RH. *J Polym Sci Polym Phys* 1997;35(12):1989–91.
- [10] Rai P, Rosen SL. *J Polym Sci Polym Phys* 1997;35(12):1985–7.
- [11] Rubinstein M, Colby RH. *Polymer physics*. Oxford University Press; 2003.
- [12] Berry GC. *J Chem Phys* 1966;44(12):4550–64.
- [13] Armarego WLF, Perrin DD. *Purification of laboratory chemicals*. 4th ed. Butterworth Heinemann; 2000.
- [14] Chu B. *Laser light scattering*. 2nd ed. New York: Academic Press; 1991.
- [15] Wu C, Zhou SQ. *Macromolecules* 1995;28(24):8381–7.
- [16] Pecora R. *Dynamic light scattering*. New York: Plenum Press; 1976.
- [17] Farnsoux B, Bouf F, Cotton JP, Daoud M, Jannink G, Nierlich M, et al. *J Phys (Paris)* 1978;39:77–86.
- [18] Weil G, des Cloizeaux J. *J Phys (Paris)* 1979;40:99–105.
- [19] Akcasu AZ, Han CC. *Macromolecules* 1979;12(2):276–80.
- [20] Brandrup J, Immergut EH, Grulke EA. *Polymer handbook*, 4th ed., Wiley-Interscience Publication.
- [21] Graessley WW, Hayward RC, Grest GS. *Macromolecules* 1999;32(10):3510–7.
- [22] Osa M, Kanda H, Yoshizaki T, Yamakawa H. *Polym J* 2007;39(5):423–7.
- [23] Curro JG, Schaefer DW. *Macromolecules* 1980;13(5):1199–203.
- [24] Schaefer DW, Curro JG. *Ferroelectrics* 1980;30:49–56.